Journal of Statistical Physics, Vol. 50, Nos. 5/6, 1988

Monte Carlo Study of Self-Avoiding Surfaces

U. Glaus[1]

Received June 2, 1987

Two models of self-avoiding surfaces on the cubic lattice are studied by Monte Carlo simulations. Both the first model with fluctuating boundary and the second one with a fixed boundary are found to belong to the universality class of branched polymers. The algorithms as well as the methods used to extract the critical exponents are described in detail. The results are compared to other recent estimates in the literature.

KEY WORDS: Self-avoiding surface; Monte Carlo; branched polymers; lattice model.

1. INTRODUCTION

In this paper two models of self-avoiding random surfaces are investigated. Random surface (RS) models have been proposed to describe a great variety of different physical phenomena. One important area is the RS expansion of lattice gauge theories.[1] This expansion creates ensembles E of RS consisting of complexes built out of the elementary 2-cells of a d-dimensional hypercubic lattice. The action of the theory then assigns the every surface S a statistical weight $Z_\beta(S)$, where β is related to the inverse gauge coupling constant. The theory of strings,[2] which currently seems to be the most promising candidate for a unified theory including quantum gravity, can be viewed as an RS theory by studying the "world sheets" created by the strings in four-dimensional space-time coordinates.

Condensed matter physics is another major area where RS models are useful. Problems involving interfaces and domain walls are usually expressed in terms of some restricted set of random surfaces; e.g., wetting,[3] roughening.[4] A RS-model may also be useful to describe membranes or sheetlike polymers in the same way as the self-avoiding walks and the

[1] Department of Physics, Clarkson University, Potsdam, New York 13676.

0022-4715/88/0300-1141$06.00/0

lattice animals are used as idealized models of linear and branched polymers.[5] Note, however, that contrary to these bond problems,[6] the RS models are generally expected to encompass a large number of different universality classes. For example, Kantor *et al.*[7] studied a RS ensemble that consists of all embeddings of a fixed two-dimensional network of "plaquettes" into d-dimensional continuous space. Such a model can be expected to behave in a rather different way from an ensemble with no restrictions on the way the elementary constituents, e.g., the plaquettes, are connected.[8] In fact, it is one of the aims of this paper to make a contribution to identifying possible universality classes of lattice models of RS.

It seems also that RS models may be a useful means to study microemulsions. Specifically, the lattice Ising model proposed by Widom[9] and recently generalized by Hofsaess and Kleinert[10] to include the Gaussian curvature term of the original continuum model due to Helfrich[11] should be an ideal candidate to investigate by the methods described in the following.

We used the Monte Carlo (MC) method to analyze the "critical behavior" of the two surface models studied. Some of our results and conclusions have already appeared in two brief reports.[12,13] RS models are usually so complex that no general analytical method has so far been developed to study them. Rigorous results are scarce and in most cases only available for RS models without any global constraints like self-avoidedness. A recent review emphasizing the mathematical aspects of RS models is Ref. 14. Other nonnumerical work on RS models is mostly rather speculative.[15,16,8] There exist a variety of MC studies of lattice models of RS,[17–20] some of them to be discussed later in relation to our results.

The paper is organized as follows. In Section 2 the two considered ensembles are defined and some facts and fictions are stated about them. The Monte Carlo methods used for each ensemble are described in two separate subsections in Section 3. All results are presented in Section 4 and a discussion of our results in relation to other work is given together with conclusions in Section 5.

2. MODELS

We consider two ensembles of self-avoiding random surface models, both defined on the hypercubic lattice Z^d. By a surface S in Z^d we understand a set of elementary 2-cells, in the following called plaquettes. Each of these plaquettes in S is supposed to be connected to at least one other plaquette of S; the word connected means here that the plaquettes share a common1-cell, i.e., a bond, in Z^d; sharing a common corner is not enough.

The bonds that belong to just one plaquette in S constitute the boundary $\partial S \equiv \gamma$ of S. The Euler characteristic χ of the surfaces is restricted to $\chi = 2$, which means that they are topologically equivalent to a sphere. Each surface is required to contain a fixed chosen plaquette p_0. The difference between the two considered ensembles consists in restrictions on the boundary ∂S as well as in the self-avoidance constraint. Specifically, these are the following.

Ensemble 1 (E_1). Consists of all surfaces whose boundary is in the set of single self-avoiding loops in Z^d. Furthermore, each plaquette, bond, and site in Z^d can be occupied at most once by S. Figure 1 shows an example of such a surface for $d = 3$.

Ensemble 2 (E_2). Includes all surfaces whose boundary is empty. The self-avoidance constraint is imposed only for the plaquettes and bonds, not for the sites in Z^d. For $d = 3$, this means that a site in Z^3 can be contained in six bonds belonging to S. A surface in this ensemble in three dimensions is depicted in Fig. 2.

We define a configuration of RS to be an equivalence class of surfaces that can be mapped onto each other by lattice translations. Let $C_{N,i}$

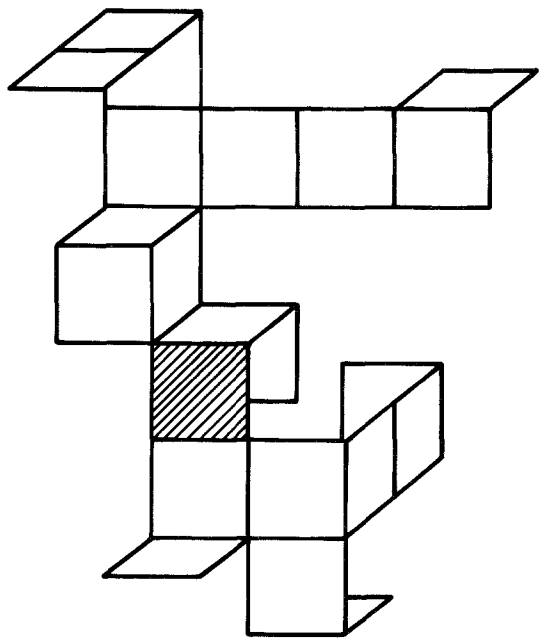

Fig. 1. A surface belonging to E_1. Hatched plaquette denotes p_0.

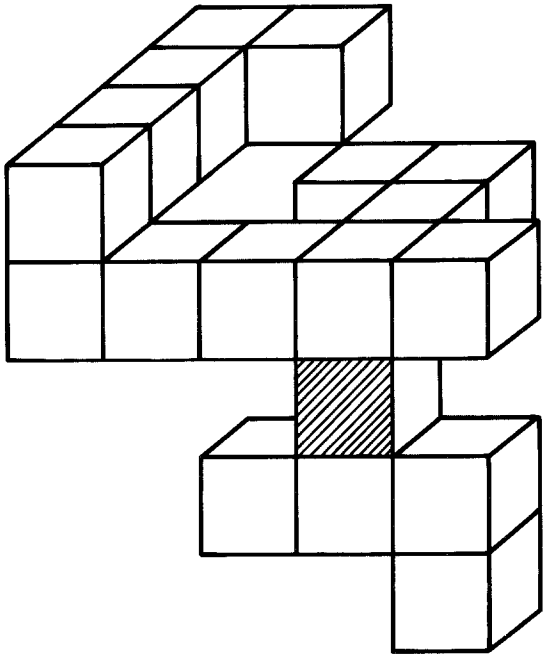

Fig. 2. Surface in E_2. Hatched plaquette denotes p_0.

$(i=1, 2)$ denote the number of configurations in E_i whose surfaces are made of N plaquettes.

Using arguments due to Hammersley,[21] Durhuus *et al.*[22] have shown that

$$\mu_2 = \lim_{N \to \infty} [C_{N,2}]^{1/N} \tag{2.1}$$

exists and is bounded by

$$[3(d-2)]^{1/4} \leqslant \mu_2 \leqslant 2d-3 \tag{2.2}$$

The same arguments can be applied to show the existence of μ_1. A crude upper bound for μ_1 is obtained by incribing a cross connecting the midpoints of opposite edges of each plaquette of $S \in E_1$. For each S, one then obtains a unique bond lattice animal containing $4N$ bonds on a hypercubic lattice of half the lattice spacing of the original lattice. From the theory of noninteracting bond nimals[23] one then gets

$$\mu_1 \leqslant (2de)^4 \tag{2.3}$$

where e is the base of the natural logarithm. By combining plaquettes in positive coordinate directions, it is easily seen that

$$2(d-1) \leqslant \mu_1 \tag{2.4}$$

Similar bounds for a related model have been obtained by Tasaki and Hara.[15] Based on analogy to the lattice geometric bond problems (e.g., the self-avoiding walk or bond lattice animals), we expect that asymptotically

$$C_{N,i} \sim \mu_i^N N^{-\theta_i} \tag{2.5}$$

as $N \to \infty$. The exponent θ_i is expected to be universal, i.e., not to depend on the lattice for a given d. However, we do not *a priori* expect that $\theta_1 = \theta_2$. Durhuus *et al.*[24] have shown that if one drops the self-avoidance constraint on the surfaces in E_2, and if $\theta_2 < 3$, then

$$\theta_2 = 5/2 \tag{2.6}$$

This value coincides with the "mean field theory" for noninteracting lattice trees and is in fact derived in an analogous way. For purely entropic reasons, almost all surfaces tend to be treelike, made up of cylindrical elements consisting of two overlapping plaquettes glued together along opposite edges. Such surfaces, when viewed from far away, look like lattice trees and it is irrelevant whether the elementary building blocks are plaquettes or bonds. The arguments in Ref. 24 obviously also apply to noninteracting surfaces in E_1 and yield therefore

$$\theta_1 = \theta_2 = 5/2 \tag{2.7}$$

As the embedding space dimensionality d tends to infinity, one can show that the self-avoidance constraint becomes irrelevant. Indeed, Drouffe *et al.*[25] have obtained $\theta_2 = 5/2$ for self-avoiding surfaces in the limit $d \to \infty$ by a mean field theory similar to the one mentioned above, except that the trees are now made out of "tubes" consisting of three-dimensional cubes with two of their six faces removed.

Another quantity of interest is the mean radius of gyration

$$R_{N,i} = \frac{1}{C_{N,i}} \sum_{\substack{S \in E_i \\ |S| = N}} R_S \tag{2.8}$$

where $|S|$ denotes the number of plaquettes in S and

$$R_S = \frac{1}{|S|} \sum_{l=1}^{|S|} \mathbf{X}_l^2 - \left(\frac{1}{|S|} \sum_{l=1}^{|S|} \mathbf{X}_l \right)^2 \tag{2.9}$$

where $\mathbf{X}_l = (x_l^1, \ldots, x_l^d)$ denotes the coordinates of the center of the lth plaquette of S. For large N, it is expected that asymptotically

$$R_{N,i} N^{\nu_i} \tag{2.10}$$

with ν_i depending only on the dimensionality d for given i. The Hausdorff or fractal dimension[26] $d_{F,i}$ of these models is related to ν_i by

$$d_{F,i} = \nu_i^{-1} \tag{2.11}$$

The "mean field theories" mentioned above yield

$$\nu_i = 1/4, \qquad i = 1, 2 \tag{2.12}$$

Since in this case $d_{F,i} = 4$, it has been argued[27] that above $d_{F,i} + d_{F,i} = 8$ dimensions, two surfaces will typically not intersect each other and the self-avoidance constraint should therefore become irrelevant, i.e., the self-avoiding surface in $d > 8$ should be correctly described by mean field theory. In low dimensions $d = 2, 3$, these arguments suggest that self-avoidance leads to non-mean-field-like critical exponents θ_i, ν_i. One purpose of the Monte Carlo simulations reported here was to check whether self-avoiding surfaces undergo a collapse into self-avoiding lattice trees even in low dimensions $d \leqslant 8$. Some support that this collapse may happen for the ensemble E_1 is given by the fact that in $d = 2$ this model is exactly dual to the ensemble of lattice animals. Heuristic arguments that this may also be true for E_2 have been brought forward by Cates.[8]

Let $p_{\mathbf{0},\mu}$ and $p_{\mathbf{x},\nu}$ denote two plaquettes in Z^d; $\mathbf{0}$ is the origin and $\mathbf{x}$ is some site in Z^d, and $1 \leqslant \mu, \nu \leqslant d(d-1)/2$ label the plaquettes attached to a given site.

Motivated by the field-theoretic description of the bond models,[28,6] we define the two-point function

$$G_i^{\mu\nu}(\mathbf{x}, \beta) = \sum_{\substack{S \in E_i \\ p_{\mathbf{0},\mu},\, p_{\mathbf{x},\nu} \in S}} \beta^{|S|} \tag{2.13}$$

and the susceptibility

$$\chi_i^{\mu}(\beta) = \sum_{\mathbf{x},\nu} G_i^{\mu\nu}(\mathbf{x}, \beta) = \sum_{\substack{S \in E_i \\ p_{\mathbf{0},\mu} \in S}} |S|\, \beta^{|S|} = \sum_{N=1}^{\infty} N^2 C_{N,i}\, \beta^N \tag{2.14}$$

$G_i^{\mu\nu}(\mathbf{x}, \beta)$ is expected, and can be shown for certain restricted ensembles of surfaces models[29] to decay exponentially in the distance $|\mathbf{x}|$ for small β. We are interested in the decay rate

$$m_i(\beta) = -\lim_{n \to \infty} n^{-1} \ln G_i^{\mu\mu}(n\mathbf{e}_l, \beta) \tag{2.15}$$

where $\mathbf{e}_l$ is a unit lattice vector ($1 \leqslant l \leqslant d$). Obviously, by symmetry, $\chi_l^{\mu}(\beta)$ does not depend on μ. From the theory of critical phenomena for spin systems we expect that there exists a "critical temperature" $\beta_{c,i}$ such that as $\beta \to \beta_{c,i}^-$

$$\chi_i(\beta) \sim (\beta_{c,i} - \beta)^{-\gamma_i} \tag{2.16}$$

$$m_i(\beta) \sim (\beta_{c,i} - \beta)^{\nu_i} \tag{2.17}$$

From (2.5), (2.14) we see that

$$\theta_i = 3 - \gamma_i, \qquad \beta_{c,i} = \mu_i^{-1} \tag{2.18}$$

and by scaling it is expected that the ν_i in (2.17) is the same as the one in (2.10). Note that in the surface model β is a plaquette activity associated with the "grand canonical" (2.14) in equilibrium with a plaquette reservoir.

3. MONTE CARLO ALGORITHMS

In thi section we describe in detail the Monte Carlo (MC) algorithms for the random surface ensembles E_1 and E_2 introduced previously. Since these are very different for the two ensembles, we describe them in two separate subsections.

3.1. MC Algorithm for E_1

Our algorithm generates surfaces in E_1 in three dimensions with the fixed plaquette p_0 in the xy plane with one corner at the origin and the remaining three corners having nonnegative coordiates. It produces surfaces in a modified grand canonical ensemble at plaquette activity β. Let γ be the self-avoiding boundary loop of a surface $S \in E_1$, i.e., $\partial S = \gamma$, and let $|\gamma|$ denote the number of bonds in γ.

A Monte Carlo step then consists in the following procedure. First a bond b is chosen at radom from the boundary loop γ. Then it either attempts to append a plaquette p_+ to S at b into one of the possible $2d-3$ directions or to remove the uniquely defind plaquette p_- that has b as one of its edges. In the former case it has to check whether the resulting surface S' as well as the new boundary loop γ' are both self-avoiding. In the latter it has to check whether γ' is still self-avoiding. To determine the Markovian dynamics, we have to specify precisely the matrix W of transition probabilities. Since at each MC step a bond is first chosen at random in γ, it follows that the number of surfaces S' that can be created from S in one MC step is proportional to $|\gamma|$; the transition probabilities from a surface S

to surface S' that can be created from S in one MC step is proportional to $|\gamma|$; the transition probabilities from a surface S to a surface S' are

$$W(S \to S') = \begin{cases} [(2d-3)\,|\tau|]^{-1}[1-c(\beta)], & S \prec S' \\ |\gamma|^{-1} c(\beta), & S' \prec S \\ [(2d-3)\,|\gamma|]^{-1}[1-c(\beta)]\,A(S) & \\ \quad + |\gamma|^{-1} c(\beta)\,B(S), & S' = S \end{cases} \tag{3.1}$$

The constant $c(\beta)$ is determined below from the detailed balance condition for the appropriate grand canonical ensemble. Here $S \prec S'$ means that S' can be constructed from S by adding a plaquette at some bond b in $\gamma = \partial S$. The integer $A(S)$ denotes the number of ways one can create a surface that violates the self-avoiding constraints by appending a plaquette at a bond in γ, and the integer $B(S)$ arises from two contributions; first, the number of ways in which γ could become non-self-avoiding by removing a plaquette from S, and second, the number of edges of p_0 that belong to γ (since p_0 should never be removed).

From the definition (3.1) of the transition probability matrix W it follows that if one requires the stationary state probabilities $P(S)$ of the Markov chain executed by the MC algorithm to be

$$P(S) = |\gamma|\,\beta^{|S|}/\Xi_1(\beta) \tag{3.2}$$

then the detailed balance equations

$$W(S \to S')\,P(S) = W(S' \to S)\,P(S') \tag{3.3}$$

reduce to [see Eq. (3.1) and (3.2)]

$$(2d-3)^{-1}[1-c(\beta)]\,\beta^{|S|} = c(\beta)\,\beta^{|S'|} \tag{3.4}$$

and hence, since $|S'| = |S| + 1$, yield

$$c(\beta) = \frac{1}{1+(2d-3)\beta} \tag{3.5}$$

The prefactor $|\gamma|$ in $P(S)$ motivates the name modified grand canonical ensemble, where in (3.2)

$$\Xi_1(\beta) = \sum_{\gamma} |\gamma| \sum_{\substack{S:\partial S=\gamma \\ S \in E_1}} \beta^{|S|} \tag{3.6}$$

It is obvious that this modification is introduced purely for computational ease, because after the algorithm has chosen a bond b at random in $|\gamma|$, it

can then proceed to compare a random number r with the *constant* $c(\beta)$. If $r \leqslant c(\beta)$, it attempts to delete a plaquette, otherwise it tries to append a plaquette at b with equal probability into one of the $2d-3$ allowed directions.

An important part in the simulation of such complex geometrical models is the design of a data structure to represent the surfaces in the computer that allows the Monte Carlo steps to be executed efficiently. We settled for a method which could be called a straightforward adaption of the data structure used to simulate self-avoiding lattice trees by Caracciolo and Glaus.[30] The design of a data structure naturally depends on the type of computer used for the simulation, which in our case was a CDC-174-721.

The surfaces are stored by specifying all the bonds $\{b_n\}_{n=1}^{N}$ they contain in the lattice. To each bond b_n we associate a link field $\{l_{n,j}\}_{j=1}^{2d}$, which has a nonzero entry only if a plaquette is appended at b_n in direction j. In this case $l_{n,j}$ contains the locations n_1, n_2, n_3 in the array $\{b_n\}$ of the three other edges of the plaquette. These are stored in consecutive bit strings within one computer word and can be retrieved by simple SHIFT and MASK operations. The bonds $\{b_{n(m)}\}_{m=1}^{M}$ that belong to γ are stored by their location $\{n(m)\}_{m=1}^{M}$ together with their directions $\{d_m\}_{m=1}^{M}$ $(1 \leqslant d_m \leqslant 2d)$. Since the MC simulation is started with $S = p_0$, the orientation of γ is fixed for all times by requiring the first step of $\gamma = \partial p_0$ from the origin to be in the direction $(1, 0, 0)$. The facilitate the upgrading, we also stored the two arrays $\{s_m^-\}_{m=1}^{M}$ ($\{s_m^+\}_{m=1}^{M}$), which contain the locations m^- (m^+) in $n(m)$ of the bonds being the backward (forward) neighbor of $b_{n(m)}$ in γ. With this data structure, the computational effort needed to complete one Monte Carlo step does not depend on the number N of bonds in S. Moreover, the storage space needed in the computer is proportional to the maximum allowed number $N_{\max}$ of bonds in S, which makes this algorithm especially suitable for a simulation in high dimensions. In Fig. 3 we draw the six essentially different "elementary moves" that are performed by the program.

In order also to keep the time for a self-avoiding check independent of $|S|$, we used two-bit maps. The follwing description is specific to a $3d$ lattice. Each lattice site is represented by a bit, which in the first map is set to one if the sete belongs to S and in the second maps is set to one if it is visited by γ. For computational reasons we only used 32 of the 60 available bits in each computer word and we reserved 2^{13} computer words for each map and therefore forced the surface to stay inside a $64 \times 64 \times 64$ lattice, which for the values of β that were used for the production runs was in fact no restriction at all on the Markov process. For some moves such as the one shown in Fig. 4 it turned out to be necessary to also perform a self-

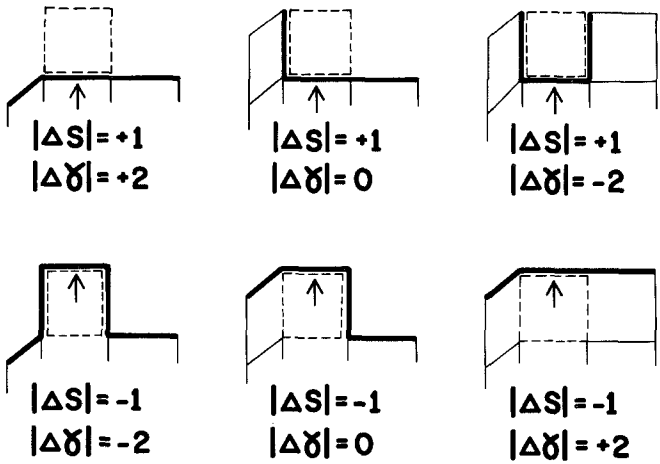

Fig. 3. The six "elementary moves" in the algorithm for E_1. The upper three moves 1–3 append the plaquette characterized by the broken-lined square. The lower three moves 4–6 remove the broken-lined plaquette. The arrow points to the randomly chosen bond in all cases. The bold-lined bonds denote the boundary $\gamma = \partial S$ of S.

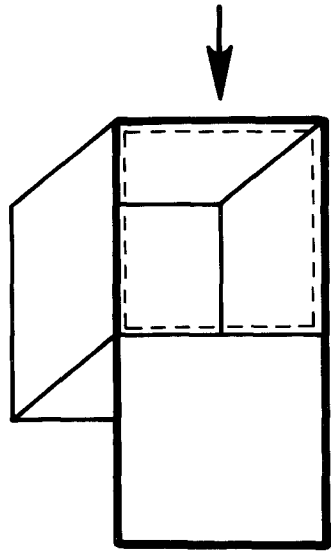

Fig. 4. A surface equivalent to a box with an open lid that necessitates the bond self-avoidance check. The algorithm attempts to add the broken-lined plaquette to the bond with the arrow in the boundary characterized by the bold lines.

avoiding check with respect to the bonds in S. The bonds were stored by their location n in $\{b_n\}$ in three additional arrays, one for each direction, of size 2^9, by using the same word for coordinates that are mapped onto each other by translations T_8 of the lattice by multiples of eight lattice spacings. Since we took $N_{\max} = 1024$, we used ten bits for each location n of the corresponding bond. This limits the size of the surface to six bonds for each set of coordinates that are equal modulo T_8; we never observed an "overflow" during the simulation. We refer to this method of storing the bonds as hash-coding.

Remark. The foregoing description of the data structure shows that the updates necessary for one successful Monte Carlo step require a rather long CPU time; we measured about 500 μsec on the CDC 174-721. It seems, however, hard to improve this significantly by a different method.

3.2. MC Algorithm for E_2

The algorithm we used to probe the ensemble E_2 is basically identical to the one proposed by Sterling and Greensite (SG)[17] with some minor, albeit crucial modifications. We will set $d = 3$ in the following. As before, the surface size $|S|$ fluctuates according to some modified grand canonical ensemble at plaquette activity β. The fixed plaquette p_0 is the same as in Section 3.1.

In this case a Monte Carlo step is more naturally described if we first briefly sketch the employed data structure. A surface S is stored in a single integer array $\{C_n\}_{n=1}^{N}$, where $N = L^3$ represents here the size of the lattice Λ used for the simulation; we chose $L = 20$. Each C_n corresponds to an elementary 3-cell or a cube in Λ; n specifies its location in Λ. If the face $p_{n,l}$ ($l = 1,..., 6$) in direction l from the center of C_n is occupied by S, then the lth bit of C_n is et to one, while it is zero otherwise. The directions are labeled as shown in Fig. 5. If, for a given surface, $C_n \neq 0$, then n is entered in a contiguous list $\{n(m)\}_{m=1}^{M}$ unless C_n is one of the two adjacent cubes sharing p_0 as one of their faces. The location m of the index n of C_n in the contiguous list $\{n(m)\}_{m=1}^{M}$ is also stored in C_n beginning at the seventh bith position.

The Monte Carlo algorithm then starts by choosing at random a cube C_n from the list $\{n(m)\}_{m=1}^{M}$ containing the indices of cubes that have faces belonging to S. It then attempts to reverse the occupied/empty status of all paquettes of C_n. In other words, its "elementary moves" consists in adding or removing the faces of cubes adjacent to S. A transition is only allowed if the resulting surface S' belongs to E_2 and if the Metropolis check for the equilibrium distribution defined below is passed.

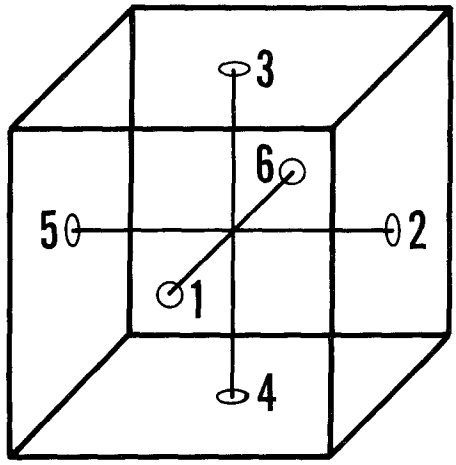

Fig. 5. The labeling of the directons of a cube.

Let $\|S\|$ denote the number of cubes with faces occupied by S. For given S and $S' \in E_2$ we then obtain the following expression for the transition probabilities:

$$W(S \to S') = \begin{cases} \dfrac{1}{\|S\| - 2}\, p(\beta, |S| \to |S'|) & S \sim S' \\ \dfrac{1}{\|S\| - 2} \left\{ \displaystyle\sum_{\substack{S' : S \sim S' \\ S' \notin E_2}} p(\beta, |S| \to |S'|) \right. & \\ \left. + \displaystyle\sum_{S' : S \sim S'} [1 - p(\beta, |S| \to |S'|] \right\} & S = S' \end{cases} \tag{3.7}$$

Here, the first term in the second line arises from the elementary moves that create a surface S' not belonging to E_2 while the second term comes from the Metropolis checks. $S \sim S'$ means that S and S' can be transformed into each other in once MC step. The factor $\|S\| - 2$ in the denominator arises from fact that a given S' can be created from S only if the right cube has been chosen among the availabe $\|S\| - 2$ that have faces in S and do not contain p_0. Clearly, the stationary state probabilities

$$P(S) = (\|S\| - 2)\, \beta^{|S|} / \Xi_2(\beta) \tag{3.8}$$

satisfy the detailed balance equations (3.3) if we choose

$$p(\beta, |S| \to |S'|) = \begin{cases} 1 & |S| \geqslant |S'| \\ \beta^{|S'| - |S|} & \text{otherwise} \end{cases} \tag{3.9}$$

The denominator in (3.8) normalizes $P(S)$ to a probability and is equal to

$$\Xi_2(\beta) = \sum_{S \in E_2} (\|S\| - 2)\, \beta^{|S|} \tag{3.10}$$

Remark 1. The only differences between this algorithm and the original one due to SG are that we keep the plaquette p_0 fixed at all times and that the upgrading is not sequential, as in SG, but random among only those cubes that are adjacent to S. We will comment later on the consequences of these modifications.

Remark 2. Since the simulation used only a lattice cube Λ of size $L = 20$ lattice spacings, it had to keep track of the maximal extension of all surfaces in all three coordinate directions; those must never exceed $L - 1$ if all surfaces in E_2 with an equal number of plaquettes are to have equal probability of occurring. Otherwise it is perfectly admissible to let a surface "spill out" of Λ and to continue it periodically into Λ again.

4. RESULTS

In this section we describe the numerical results obtained by extensive simulations of the MC algorithms. A major effort was spent to estimate statistical and systematic errors as carefully as possible; in this we followed the Monte Carlo work by Berretti and Sokal[31] on the two-dimensional self-avoiding walk. Some peculiarities arising for observable averages due to the prefactors $|\gamma|$ (resp. $\|S\|$) in the modified grand canonical ensembles Ξ_1 (resp. Ξ_2) will also be pointed out.

4.1. Results for the Ensemble E_1

The runs for this ensemble were performed on a CDC Cyber 174-721 at the Rechenzentrum of the ETH in Zurich, Switzerland. Since the implementation of the algorithm for E_1 is very complex, we performed numerous checks with the program before starting the production run. During the run we checked every 2×10^6 MC iterations whether the surface still belonged to E_1. Since this was the case during the total of 2.5×10^9 iterations, we are confident that the program contains no error.

The methods described in Ref. 31 allow one to extract information about the exponents θ_1 and ν_1 and the "growth constant" μ_1 from a simulation of the grand canonical ensemble Ξ_1 at one single activity β. We took

$$\beta = 0.074 \tag{4.1}$$

which was determined to be optimal from some preliminary runs. Note that it follows from (2.5) and (3.2) that as $\beta \to \beta_{c,1}$, one gets approximately

$$\frac{\langle |S|/|\gamma| \rangle}{\langle 1/|\gamma| \rangle} \sim \frac{\beta(2-\theta_1)}{\beta_{c,1}-\beta} \tag{4.2}$$

Here the brackets $\langle\ \rangle$ denote expectations with respect to the probability (3.2); the average size of $|S|$ can therefore be set to any desired value by appropriately choosing β.

It is seen in Eq. (4.2) that we had to take the ratio of the expectations for $|S|/|\gamma|$ and $1/|\gamma|$ in order to relate the mean surface size to (2.5). This arises from the factor $|\gamma|$ in $P(S)$, (3.2). In fact, we can obtain the expectation for any observable O on E_1 with respect to the unmodified grand canonical probability measure

$$P_0(S) = \beta^{|S|} \Big/ \sum_{S \in E_l} \beta^{|S|} \tag{4.3}$$

simply by calculating the ratio

$$\langle O(S)/|\gamma| \rangle / \langle |\gamma|^{-1} \rangle \tag{4.4}$$

with the probability (3.2).

The program was left running for a total of 2.5×10^9 MC iterations starting with the surface consisting of the single plaquette p_0. Every 5×10^3 MC steps the number of bonds B_S, the number of boundary links $|\gamma|$, and the radius of gyration R_S were measured. Every 500 measurements these data were stored on tape for the subsequent statistical analysis. In addition to the surface observables, we also recorded the acceptance fraction F as well as the fractions F_{SA}, F_{LA} of unsuccessful attempts to change a surface S to S' due to S' not being self-avoiding (F_{SA}) or $\gamma' = \partial S'$ not being self-avoiding (F_{LA}). The fraction F_{DIS} of attempts that would result in a disconnected S' was also recorded. Note that the transition probabilities (3.1) are chosen such that at each MC step an attempt to either remove or add a plaquette is actually made.

The values for the acceptance/rejection rates are listed in Table I. The

Table I. Acceptance and Rejection Rates As Explained in Text

Acceptance rate, %	Rejection rate, %
$F = 35.1$	$F_{SA} = 4.1$ $F_{LA} = 39.6$ $F_{DIS} = 21.2$

quoted values are accurate to at least the last given digit. Surprisingly, these values indicate that only 4.1% of all MC steps attempt to create a surface that violates the self-avoiding constraint. It is much more likely to have a collision of the boundary loop γ or to dissect a surface into two pieces. This is a first indication that typical surfaces in E_1 are ramified this structures consisting primarily of branches of single plaquettes glued together at two edges and that only a negligible fraction of surfaces cover a large compact area.

For a correct treatment of the statistical errors due to the finite sampling of E_1 in the MC simulation, it is necessary to have an estimate of the autocorrelation time of the algorithm. For this purpose we have estimated the autocorrelation functions $C_{00}(s)$ of the observables $O=|S|$ and $O=R_S$ by using the estimator

$$\hat{C}_{oo}(s)=\frac{1}{n-|s|}\sum_{t=1}^{n-|s|} O_t O_{t+s}-\langle O\rangle^2 \tag{4.5}$$

where O_t denotes the value of O at the tth measurement and the sample size n is in our case

$$n=(2.5\times 10^9)/(5\times 10^3)=5\times 10^5$$

For the average $\langle O\rangle$ we use the natural estimator

$$\langle O\rangle=\frac{1}{n}\sum_{t=1}^{n} O_t \tag{4.6}$$

Since it can be shown[31] that for our MC algorithm $C_{oo}(s)$ has the form

$$C_{oo}(s)=\sum_j \alpha_j^o \exp(-\lambda_j^o s) \tag{4.7}$$

with $0<\lambda_1^O<\lambda_2^O,\ldots$, it follows that λ_1^O sets the time scale needed for a given observable O to lose its memory; we therefore take

$$\tau_{oo}=[\lambda_1^O]^{-1}$$

as the autocorrelation time for O and estimate it from plotting

$$\tau_{oo}(s)=\frac{-|s|}{\ln[C_{oo}(s)/C_{oo}(0)]} \tag{4.8}$$

as a function of s and extrapolating s to infinity. Figure 6 plots $\tau_{|S|,|S|}(s)$ and $\tau_{R_S,R_S}(s)$ versus s. Note that in both cases the data become noisy for

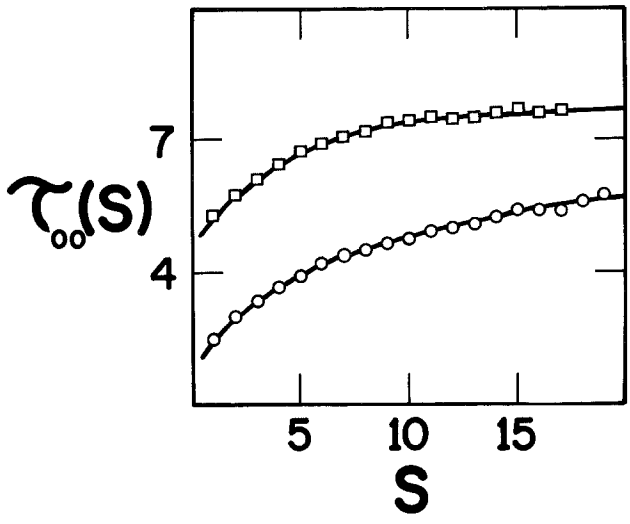

Fig. 6. Autocorrelation times $\tau_{oo}(s)$ [eq. (4.8)] for $O = S(\cdot)$ and $O = R_S(\cdot)$ versus s. The τ's are in measured units, each unit corresponding to 5000 MC steps.

$s \geqslant 15$ (corresponding to 75,000 MC iterations). It is clearly seen, however, that these curves behave as predicted by (4.7) and we estimate

$$\tau_{|S|,|S|} = (2.8 \pm 0.3) \times 10^4 \text{ MC Steps} \tag{4.9}$$

$$\tau_{R_S,R_S} = (3.8 \pm 0.5) \times 10^4 \text{ MC Steps} \tag{4.10}$$

where we obtained the error bars from the crude estimate

$$\Delta \hat{C}_{oo}(s) \leqslant \frac{2\tau_{oo}}{n} C_{oo}^2(0) \tag{4.11}$$

The statistical error bars therefore, as will be the case in all later estimates, represent the classical 95% confidence limits. For later statistical error estimates τ_{R_S,R_S} was taken for the autocorrelation time τ of the MC algorithm. The means [eq. (4.6)] of $|\gamma|$, B_S, and $|S|$ were found to be

$$\begin{aligned} \langle |\gamma| \rangle &= 56.10 \pm 0.38 \\ \langle B_S \rangle &= 84.50 \pm 0.58 \\ \langle |S| \rangle &= (2B_S - |\gamma|)/4 = 28.04 \pm 0.20 \end{aligned} \tag{4.12}$$

For the following analysis we define the "censored mean" of an observable O to be

$$\langle O \rangle_{N_{\min}} = \sum_{t=1}^{n} O(S_t)\, \chi(|S_t| \geqslant N_{\min}) \Big/ \sum_{t=1}^{n} \chi(|S_t| \geqslant N_{\min}) \tag{4.13}$$

where χ is the characteristic function for the event $|S_t| \geqslant N_{\min}$. Only surfaces with at least $N_{\min}$ plaquettes are used to calculate $\langle O \rangle_{N_{\min}}$; this is useful to get a feeling for the corrections to scaling by observing the behavior of $\langle O \rangle_{N_{\min}}$ as a function of $N_{\min}$.

An interesting observable for E_1 is the ratio $|S|/|\gamma|$. By extrapolating $\langle |S|/|\gamma| \rangle_{N_{\min}}$ to $N_{\min} \to \infty$ we obtain the estimate

$$\langle |S|/|\gamma| \rangle = 0.515 \pm 0.01 \pm 0.003 \tag{4.14}$$

for this ratio. Here, as later, the first term on the right side refers to our central estimate, the second to our estimate of the systematic error due to corrections to scaling, and the last gives the statistical error [twice variance times $(2\tau)^{1/2}$], which is very small, indicating little fluctuation in this quantity. Moreover, our central estimate is finite and very close to 1/2, which implies that the plaquettes contribute on the average two of their edges to the boundary loop $|\gamma|$. Therefore, typical surfaces are ramified treelike structures with almost all plaquettes having edges at the boundary ∂S.

The estimates for θ_1 and μ_1 were obtained by means of the maximum likelihood method. Based on Eq. (2.5), we took into account the effects due to corrections to scaling by assuming that for $N \geqslant N_{\min}$, we have exactly

$$C_{N,1} = \mu_1^N N^{-\theta_1}(1 + a/N) \tag{4.15}$$

This is admittedly a very crude way to treat these corrections. A nonanalytic term b/N^{ω} with $\omega < 1$ should in general be expected and would clearly dominate the large-N behavior of the corrections. By te same reasoning one would also have to take into account a multitude of further analytic and nonanalytic corrections to scaling terms with unknown amplitudes. It seems hopeless to disentable these with the available data and we feel that (4.15) is jsut as good as any other Ansatz; it merely serves to obtain a crude estimate for the order of magnitude of these corrections by varying $N_{\min}$ and a and recording the resulting behavior of θ_1 and μ_1. Once can thereby determine a subjective estimate of the systematic error for the exponents due to these corrections. We think that a systematic error estimate should be represented in such a way that it is easy for everyone to check and see whether it meets his or her individual standards.

The maximum likelihood method then amounts to equating, for the observables $O(|S|) = |S|$ and $O(|S|) = \ln |S|$, the "theoretical averages"

$$\langle O \rangle_{N_{\min}} = \left[\sum_{N=N_{\min}}^{\infty} O(N)\, NC_{N,1} \right] \left[\sum_{N=N_{\min}}^{\infty} NC_{N,1} \right]^{-1} \tag{4.16}$$

to the observed averages $\langle O/|\gamma| \rangle_{N_{\min}} / \langle 1/|\gamma| \rangle_{N_{\min}}$. For each pair $(N_{\min}, a)$

one can thus obtain $\theta_1(N_{\min}, a)$ and $\mu_1(N_{\min}, a)$ by solving numerically the two equations for $O = |S|$ and $O = \ln |S|$.

In Fig. 7, θ_1 and μ_1 are plotted versus $N_{\min}^{-1}$ for various a. From this plot we estimate

$$\theta_1 = 1.48 \pm 0.12 \pm 0.05 \tag{4.17}$$

$$\mu_1 = 12.798 \pm 0.025 \pm 0.018 \tag{4.18}$$

The statistical error here is twice the variance for $N_{\min} = 20$ obtained from the explicitly known covariace matrix multiplied by $(2\tau)^{1/2}$. For the estimation of ν_1, we minimized the expression

$$\varepsilon(\nu_1, b_0) = \langle [\ln R_S - \nu_1 \ln(|S| + b_1) + b_0]^2 \rangle_{N_{\min}}$$

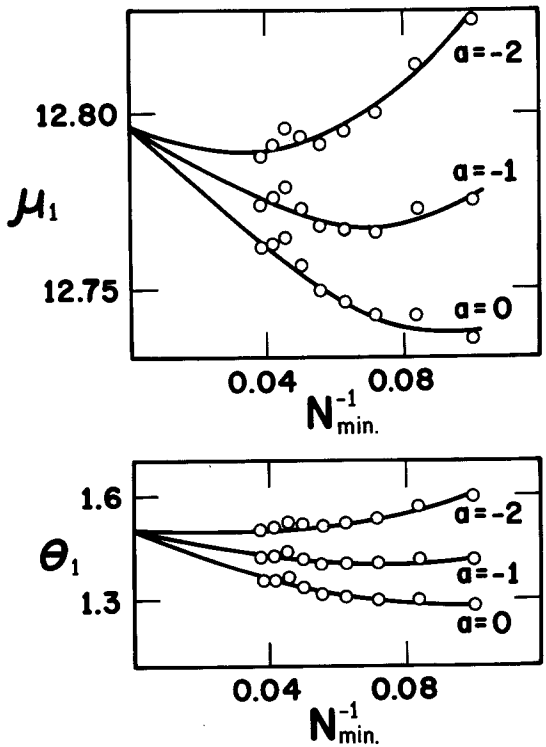

Fig. 7. Plot of μ_1 (top) and θ_1 (bottom) versus $N_{\min}^{-1}$ for various a. Circles denote measured values, which show statistical fluctuations. The lines are guides to the eye that were used to obtain the central estimates.

with respect to ν_1 and b_0 for various b_1 and $N_{\min}$. The results for ν_1 are plotted against $N_{\min}^{-1}$ in Fig. 8 and we estimate

$$\nu_1 = 0.504 \pm 0.010 \pm 0.0006 \tag{4.19}$$

The statistical error is twice the variance from least squares theory (for $N_{\min} = 40$) multiplied by $(2\tau)^{1/2}$. Note that both θ_1 and ν_1 are close to the exact branched ploymer values $\theta = \frac{3}{2}$, $\nu = \frac{1}{2}$,[32] and together with the quoted error bars are certainly consistent with them.

4.2. Results for E_2

The runs for E_2 were performed on the Cyber 205 at the National Bureau of Standards in Gaitherburg, Maryland, where one MC step required about 45 μsec.

The production run was performed with the fixed activity β set at

$$\beta = 0.56 \tag{4.20}$$

It started with a single cube containing p_0 and comprised a total of 10^8 MC steps. In order to be able to compare the MC results to the theoretical expectation (2.5), averages of O should be performed with respect to the unmodified probability measure (4.3), which from (3.8) can be seen to correspond to take the ratio

$$\langle O/(\|S\| - 2)\rangle / \langle 1/(\|S\| - 2)\rangle \tag{4.21}$$

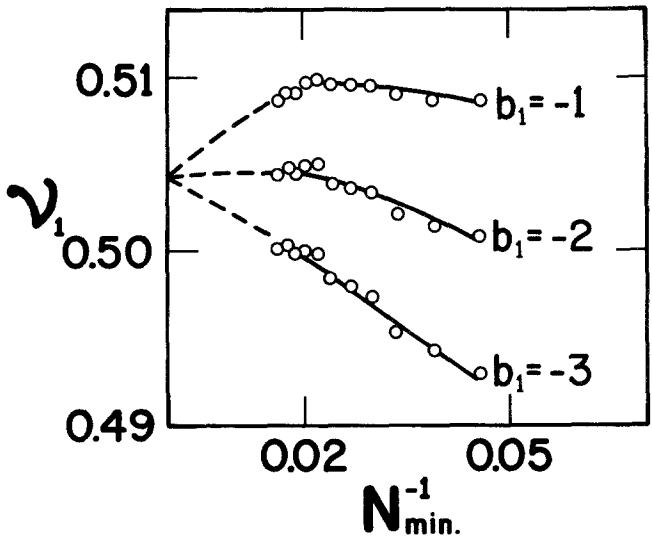

Fig. 8. Plot of ν_1 versus $N_{\min}^{-1}$ for various b_1. Lines are guides to the eye.

Data were taken every 2×10^3 MC steps. They consisted of the number of plaquettes $|S|$, the volume V_S enclosed by S, and R_S. The acceptance fraction was not recorded for this algorithm. Using the previously described method, we measured an autocorrelation time

$$\tau = (5.6 \pm 0.8) \times 10^3 \text{ MC Steps} \tag{4.22}$$

for this run. The means of $|S|$ and V_S are

$$\langle |S| \rangle = 50.26 \pm 0.40 \tag{4.23}$$

$$\langle V_S \rangle = 13.50 \pm 0.15 \tag{4.24}$$

The analog to $\langle |S|/|\gamma| \rangle_{N_{\min}}$ for E_1 is naturally $\langle |S|/V_S \rangle_{N_{\min}}$ for E_2 [see (4.13) for the definition of $\langle \ \rangle_{N_{\min}}$]. For $N_{\min} \to \infty$, we estimate

$$\langle |S|/V_S \rangle = 3.50 \pm 0.010 \pm 0.005 \tag{4.25}$$

Again this ratio shows very little fluctuation and is finite, which implies that $|S|$ is typically proportional to V_S, and from the estimate (4.25) one concludes that the surfaces in E_2 are made of tubes consisting of single cubes with two of their faces removed so they are very ramified and treelike.

The corrections to scaling for μ_2 and θ_2 were taken into account in the same way as for E_1 and the resulting estimates are

$$\theta_2 = 1.51 \pm 0.10 \pm 0.15 \tag{4.26}$$

$$\mu_2 = 1.733 \pm 0.005 \pm 0.006 \tag{4.27}$$

and for ν_2 we estimate

$$\nu_2 = 0.502 \pm 0.012 \pm 0.012 \tag{4.28}$$

Again, both θ_2 and ν_2 are close to the branched ploymer values $\theta = 3/2$, $\nu = 1/2$ and consistent with them.

5. DISCUSSION

5.1. Comparsion to Previous Work

If we compare our results for θ_i, ν_i, and μ_i to estimates of these quantities on similar or idential models obtained by other authors with a variety of methods, we find a surprisingly large number of inconsistencies. We believe it is important to discuss these discrepancies in some detail and to

point out the subtleties involved in a correct implementation of an MC simulation of a random surface model.

We discuss two papers that consider surfaces related to the ensemble E_1. First there is Redner's[33] exact enumerration study of self-avoiding surfaces on the cubic lattice Z^3 with up to ten plaquettes. In Redner's model the boundary need not be connected, nor does he impose any restriction on the genus. Our proof of exponential boundedness naturally carries over to his model as well. His estimates

$$\theta = 1.5 \tag{5.1}$$

$$\nu = 0.538 \pm 0.03 \tag{5.2}$$

agree well with ours. Redner also finds that the average number of boundary bonds $\langle |\gamma| \rangle_N$ for all surfaces with N plaquettes varies linearly with N and gives approximately

$$\langle |\gamma| \rangle_N / N \sim 2.3 \tag{5.3}$$

in reasonable agreement with (4.14), although his model is different from ours.

Another ensemble closely related to E_1 is the connected plaquette model of Tasaki and Hara.[15] Their only restrictions are, however, that the surfaces S have to be connected and their notion of boundary seems somewhat arbitrary. Nevertheless, they prove an exponential bound [see Eq. (2.3)] for their model and provide an appealing argument suggesting, in agreement with our results, that the model should collapse into branched polymers in the scaling limit.

A considerable amount of MC work has been devoted to surface models identical or closely related to E_2. Sterling and Greensite (SG)[17] originally studied the ensemble E_2 with a grand canonical MC simulation by varying the plaquette activites β, with partition function

$$\Xi_{SG}(\beta) = \sum_{S \in \tilde{E}_2} \beta^{|S|} \tag{5.4}$$

Note the missing factor $(\|S\| - 2)$ compared to $\Xi_2(\beta)$, (3.8), which arises only when cubes adjacent to S are accessed at random. Moreover, the ensemble considered by SG is not exactly identical to E_2, since there is no fixed plaquette p_0 in their simulation. This implies that the probability for a surface S with N plaquettes to occur in the MC run in equilibrium is

$$P_{SG}(|S| = N) = \frac{C_{N,2}\beta^N}{\sum_{|M|=6}^{\infty} C_{M,2}\beta^M} \tag{5.5}$$

In our simulation, this probability is proportional to

$$P(|S| = N) \sim N^2 C_{N,2} \beta^N / \Xi_2(\beta) \tag{5.6}$$

because of Eq. (3.8) and the fact that $\|S\| \sim |S|$, yielding a factor N in (5.6), and because p_0 is kept fixed and $C_{N,2}$ counts only the different configurations, there is another factor N.

If we use the asymptotic behavior (2.5) for $C_{N,2}$ with our estimate (4.26) for θ_2, we find that for $\beta < \beta_{c,2}$, P_{SG} is primarily concentrated at small values of N. This means that for the original SG algorithm a lot of simulation time is wasted for creating small surfaces that will be discraded anyway in the data analysis [see our definition (4.13) of $\langle O \rangle_{N_{\min}}$]. By contrast, the probability (5.6), since

$$2 - \theta_2 > 0 \tag{5.7}$$

will have a maximum at

$$N(\beta) = \frac{\theta_2 - 2}{\ln(\mu_2 \beta)} \tag{5.8}$$

and $N(\beta) \to \infty$ as $\beta \to \beta_{c,2}$.

Therefore, our algorithm, once equilibrated, will be

$$\frac{P(|S| = N(\beta))}{P(|S| = 6)} = \frac{(\beta_{c,2} - \beta)^{\theta - 2} \, e^{(\theta - 2)[1 - \ln(2 - \theta) + \ln \mu]}}{36 \beta^6} \tag{5.9}$$

more likely to produce a surface of size $N(\beta)$ than a single cube with six plaquettes. For our production run at $\beta = 0.56$ this corresponds to

$$\frac{P(|S| = N(\beta))}{P(|S| = 6)} \approx 2.4 \tag{5.10}$$

while the same ratio for the SG algorithm at $\beta = 0.56$ is

$$\frac{P_{SG}(|S| = N(\beta))}{P(|S| = 6)} \approx 0.28 \tag{5.11}$$

This calculation clearly demonstrates that our modifications render the SG algorithm much more efficient. We actually tested these expectations for both the original SG algorithm and our modified version by monitoring the distributions $P(|S| = N)$ and $P_{SG}(|S| = N)$ during test runs. They both behaved exactly according to the foregoing analysis. Of course, the low ratio (5.11) could be avoided by simulating at an activity $\beta > \beta_{c,2}$. Then

$P_{SG}(|S|=N)$ would no longer be normalizable and it would have a minimum at

$$\tilde{N}(\beta)=\frac{\theta_2}{\ln \mu_2 \beta} \tag{5.12}$$

after which it increases exponentially. One could then introduce a cutoff $N_{\max} \gg \tilde{N}(\beta)$ and never allow a surface with $|S|>N_{\max}$. However, since P is then so strongly concentrated at $N_{\max}$, it will be hard to extract information about θ_2 and μ_2 from this essentially microcanonical ensemble. In fact, SG ran their algorithm at activities β larger than our estimate of $\beta_{c,2}$. But since each run was started at the surface consisting of a single elementary cube, the surface size presumably never got larger than $\tilde{N}(\beta)$ and it always stayed in the "metastable region" $N<\tilde{N}(\beta)$. Another way to circumvent the problem of low efficiency in the SG algorithm is to change the grand canonical ensemble to

$$\Xi_k(\beta)=\sum_{S\in E_2} \beta^{|S|+k \ln |S|/\ln |\beta|}=\sum_{S\in E_2} |S|^k \beta^{|S|} \tag{5.13}$$

which can easily be achieved by changing the transition probabilities W. Any desired power $|S|$ can be obtained with this method.

Moreover, in order to estimate θ_2 and μ_2, SG measured the average size $\langle |S| \rangle$ of a MC run at various values of β. According to (5.5) and (2.5), for fixed β this is expected to be given by

$$\langle |S| \rangle = \left[\sum_{N=6}^{\infty} N^{1-\theta_2}(\beta\mu)^N\right] \Big/ \Xi_{SG}(\beta) \tag{5.14}$$

Replacing the sums by integrals and extending the lower limit of the integrals to 0, the rhs of (5.14) can be approximately replaced by

$$\langle |S| \rangle \sim \frac{1-\theta_2}{1-\beta\mu_2} \tag{5.15}$$

provided that $\theta_2<1$. Plotting $\langle |s| \rangle^{-1}$ versus β, they found

$$\theta_2 = 0.5 \pm 0.05 \tag{5.16}$$

$$\mu_2 = 1.701 \pm 0.005 \tag{5.17}$$

in contradiction to our values (4.26), (4.27), especially for θ_2. We believe that our estimates are more accurate because (i) our method for estimating θ_2 does not involve any *a priori* assumptions, while SG had to assume

$\theta_2 < 1$, and (ii) our algorithm is not becoming "metastable" as β gets larger than $\beta_{c,2}$. Instead, it indicates the approach of β to $\beta_{c,2}$ from below by producing larger and larger surfaces that eventually no longer fit into Λ.

An interesting simulation of planar random surfaces without spikes (PRSWS) in Z^4 is due to Baumann and Berg.[18] Their algorithm is quite different from SG's and does not store the whole lattice in the computer, but only the part occupied by the surface. PRSWS are only locally self-avoiding, e.g., no two plaquettes of a PRSWS are allowed to occupy the same 2-cell in Z^4. These authors note the problems with creating primarily small surfaces for $\beta < \beta_c$ and perform most of their runs for $\beta > \beta_c$. They found for their model

$$\theta = 2.74 \pm 0.03 \tag{5.18}$$

$$\nu = 1/4 \tag{5.19}$$

$$3.25 < \mu < 3.3 \tag{5.20}$$

in contrast to the PRS result (2.5) that $\theta = 5/2$. This result also contradicts our contention that a global self-avoiding constraint only changes the universality class of an RS model from noninteracting branched polymers to ordinary branched polymers, which implies that θ should be equal to 5/2 for the PRSWS model. We believe that their estimate may be wrong because the constant $C_{\beta_2}^{\beta_1}$ in their Eq. (10) actually is equal to

$$C_{\beta_2}^{\beta_1} = e^{\beta_c(A_2 - A_1)} \tag{5.21}$$

and therefore involves an estimate of β_c. These two quantities should not be estimated independently from each other, as they are highly correlated. Finally, there is some recent MC work using the SG algorithm by Karowski,[19] who considers, among other models, also the ensemble E_2 and estimates

$$\nu_2 = 0.435 \pm 0.022 \tag{5.22}$$

in agreement with a Flory argument for self-avoiding surfaces due to Maritan and Stella.[16] However, the method he uses to estimate ν_2 is quite complicated and from Fig. 16 in Ref. 19 it seems clear that the error bar should be increased by at least a factor three, making his estimate consistent with $\nu_2 = 1/2$. Moreover, the correct Flory theory for all these surface models seems to us to be the one due to Lubensy and Isaacson for branched polymers, in line with all our results.

5.2. Conclusions

In this paper we presented two models of self-avoiding random surfaces and analyzed them by means of the Monte Carlo method in three dimensions. We pointed out that the implementation of correct and efficient MC methods is a rather tricky problem for such complex geometrical models. Our results for the "critical exponents" indicate that both surface models belong to the universality class of branched polymers for which the exponents in $d=3$ are known exactly to be $\theta=3/2$, $\nu=1/2$.[32] Thus, our conclusion is that any lattice random surface model with short-range repulsive interactions will belong to this universality class. The reason, as pointed out previously by other authors,[8,15] is that treelike thin surfaces have such a high entropy that they dominate the critical behavior even in the lowest nontrivial dimension $d=3$.

The method[31] we used to extract the exponent estimates from the data turned out to be very efficient. We believe that this is the reason that our estimates are at variance with practically all other Monte Carlo work on identical or almost identical models of random surfaces.[17-19] This is only partly due to the fact that the field is relatively new and that there are a multitude of possibilities to define a random surface model.

Finally, our simulations have indicated that the SG algorithm, if handled with care, is very useful for studying physical problems involving lattice random surfaces in three dimensions. We intend to apply it in the near future to the Widom model[9] for microemulsions.

ACKNOWLEDGMENTS

I thank S. Caracciolo, T. Einstein, J. Froelich, and especially A. Sokal for providing useful insights during various stages of this work. I also thank the staff of the Rechenzentrum of the ETH Zurich, Switzerland, and J. Amar of the NBS Gaithersburg, Maryland, for providing assistance in the use of the computers there. This work was supported in part by the Swiss National Science Foundation and in part by the Department of Energy under grant DE-FG 05-84ER45071.

REFERENCES

1. R. Balian, J. M. Drouffe, and C. Itzykson, *Phys. Rev. D* **11**:2104 (1975).
2. A. Polyakov, *Phys. Lett.* **103B**:207 (1981).
3. P. G. de Gennes, *Rev. Mod. Phys.* **57**:827 (1985).
4. H. J. Leamy, G. H. Gilmer, and K. A. Jackson, in *Surface Physics of Crystalline Materials*, J. M. Blakely, ed. (Academic Press, New York, 1976).

5. P. G. de Gennes, *Scaling Concepts in Polymer Physics* (Cornell University Press, Ithaca, New York, 1979).
6. P. G. de Gennes, *Phys. Lett.* **38A**:339 (1972); T. C. Lubensky and J. Isaacson, *Phys. Rev. A* **20**:2130 (1979).
7. Y. Kantor, M. Kardar, and D. R. Nelson, *Phys. Rev. Lett.* **57**:791 (1986), and Harvard preprint.
8. M. E. Cates, *Phys. Lett.* **161B**:363 (1985).
9. B. Widom, *J. Phys. Chem.* **88**:6508 (1984); *J. Chem. Phys.* **84**:6943 (1986).
10. T. Hofsaess and H. Kleinert, *J. Chem. Phys.* **86**:3565 (1987).
11. W. Nelfrich, *Z. Naturforsch. B* **103**:67 (1975).
12. U. Glaus, *Phys. Rev. Lett.* **56**:1996 (1986).
13. U. Glaus and T. L. Einstein, *J. Phys. A* **20**:L105 (1987).
14. J. Froehlich, in *Applications of Field Theory to Statistical Mechanics*, L. Garrido, ed. (Lecture Notes in Physics, Vol. 216, Springer, Berlin, 1985).
15. H. Tasaki and T. Hara, *Phys. Lett.* **112A**:115 (1985).
16. A. Maritan and A. Stella, *Phys. Rev. Lett.* **53**:123 (1984).
17. T. Sterling and J. Greensite, *Phys. Lett.* **121B**:345 (1983).
18. B. Baumann and B. Berg, *Phys. Lett.* **164B**:131 (1985).
19. M. Karowski, *J. Phys. A* **19**:3375 (1986).
20. B. Berg and A. Billoire, *Phys. Lett.* **139B**:297 (1984); R. Schrader, *J. Stat. Phys.* **40**:533 (1985); M. Karowski and H. J. Thun, *Phys. Rev. Lett.* **54**:2556 (1985).
21. J. M. Hammersley, *Proc. Camb. Phil. Soc.* **57**:516 (1961).
22. B. Durhuus, J. Froehlich, and T. Jonsson, *Nucl. Phys. B* **225**:185 (1983).
23. A. Bovier, J. Froehlich, and U. Glaus, in *Critical Phenomena, Random Systems and Gauge Theories* (Les Houches, Sesion XLIII), K. Osterwalder and R. Stora, eds. (Elsevier, Amsterdam, 1986).
24. B. Durhuus, J. Froehlich, and T. Jonsson, *Nucl. Phys. B* **240**:453 (1984).
25. J. M. Drouffe, G. Parisi, and N. Sourlas, *Nucl. Phys. B* **161**:397 (1980).
26. B. B. Mandelbrot, *Fractals: Form Chance and Dimension* (Freeman, San Francisco, 1977); *The Fractal Geometry of Nature* (Freeman, San Francisco, 1982).
27. G. Parisi, *Phys. Lett.* **81B**:357 (1979).
28. K. Symanzik, Euclidean quantum field theory, in *Local Quantum Theory*, R. Jost, ed. (Academic Press, New York, 1969); D. Brydges, J. Froehlich, and T. Spencer, *Commun. Math. Phys.* **83**:123 (1982).
29. D. B. Abraham, J. T. Chayes, and L. Chayes, *Commun. Math. Phys.* **96**:439 (1984).
30. S. Caracciolo and U. Glaus, *J. Stat. Phys.* **41**:95 (1985).
31. A. Berretti and A. Sokal, *J. Stat. Phys.* **40**:483 (1985).
32. G. Parisi and N. Sourlas, *Phys. Rev. Lett.* **46**:871 (1981).
33. S. Redner, *J. Phys. A* **18**:L723 (1985), **19**:3199 (1986).